Clinical Neurophysiology 129 (2018) 1669–1679

Contents lists available at ScienceDirect

Clinical Neurophysiology

journal homepage: www.elsevier.com/locate/clinph

# Central neuropathic pain in paraplegia alters movement related potentials

Aleksandra Vučković [a,*], Mohammed Jarjees [a,b], Muhammad Abul Hasan [a,c], Makoto Miyakoshi [d], Matthew Fraser [e]

[a] Centre for Rehabilitation Engineering, Biomedical Engineering Division, School of Engineering, University of Glasgow, Glasgow, UK
[b] Technical Engineering College of Mosul, Northern Technical University, Mosul, Iraq
[c] Department of Biomedical Engineering, NED University of Engineering and Technology, Karachi, Pakistan
[d] Swartz Center for Computational Neuroscience, University of California, CA, USA
[e] Queen Elizabeth National Spinal Injuries Unit, Queen Elizabeth University Hospital, Glasgow, UK

ARTICLE INFO

*Article history:*
Accepted 28 May 2018
Available online 15 June 2018

*Keywords:*
Central neuropathic pain
Spinal cord injury
Movement related cortical potentials
Event related potentials
Motor imagery
Measure projection analysis

HIGHLIGHTS

- Central neuropathic pain dominantly influences movement related cortical potentials in a domain comprising the limbic system.
- Both pain and paralysis affect the reafferentation potential, which is delayed.
- Central neuropathic pain influences cognitive processes in a domain specific manner.

ABSTRACT

*Objectives:* Spinal Cord Injured (SCI) persons with and without Central Neuropathic Pain (CNP) show different oscillatory brain activities during imagination of movement. This study investigates whether they also show differences in movement related cortical potentials (MRCP).
*Methods:* SCI paraplegic patients with no CNP ($n = 8$), with CNP in their lower limbs ($n = 8$), and healthy control subjects ($n = 10$) took part in the study. EEG clustering involved independent component analysis, equivalent current dipole fitting, and Measure Projection to define cortical domains that have functional modularity during the motor imagery task.
*Results:* Three domains were identified: limbic system, sensory-motor cortex and visual cortex. The MRCP difference between the groups of SCI with and without CNP was reflected in a domain located in the limbic system, while the difference between SCI patients and control subjects was in the sensori-motor domain. Differences in MRCP morphology between patients and healthy controls were visible for both paralysed and non paralysed limbs.
*Conclusion:* SCI but not CNP affects the movement preparation, and both SCI and CNP affect sensory processes.
*Significance:* Rehabilitation strategies of SCI patients based on MRCP should take into account the presence of CNP.


## 1. Introduction

Central Neuropathic Pain (CNP) is caused by an injury to the somatosensory system (Jensen et al., 2011) affecting more than 40% Spinal Cord Injured (SCI) patients (Siddall, 2003). The cortical activity of SCI patients is thus affected by both CNP and paralysis (Boord et al., 2008, Vuckovic et al., 2014). To understand the effect of SCI on EEG during motor tasks, researchers have analysed

*Abbreviations:* CNP, Central Neuropathic Pain; SCI, spinal cord injury; MI, motor imagery; AB, able bodied; PwP, patients with pain; PnP, patients without pain; MRCP, movement related cortical potentials; ERS/ERD, event related synchronisation/desynchronisation; ERP, event related potentials; ASIA, American Spinal Injury Association; VAS, Visual Numerical Scale.

* Corresponding author at: Biomedical Engineering, School of Engineering, James Watt (South) Building, University of Glasgow, G12 8QQ Glasgow, UK.
*E-mail address:* Aleksandra.vuckovic@glasgow.ac.uk (A. Vučković).

https://doi.org/10.1016/j.clinph.2018.05.020
1388-2457/

both event-related synchronisation/desynchronisation (ERS/ERD) (Pfurtscheller et al., 2009) and movement related cortical potential (MRCP) (Castro et al., 2013). Because CNP and SCI are different phenomena and have different cortical substrata, the effect of SCI on CNP has been investigated using ERS/ED and MRCP. MRCP is a subtype of Event Related Potential (ERP) and presents the type of post-synaptic responses of main pyramidal neurons (Shibasaki et al., 1980, Luck, 2005) triggered by an overt or covert motor action while ERS/ERD present changes in parameters that control oscillations in neuronal networks (Pfurtscheller and Lopes da Silva, 1999). Pfurtscheller et al. (2009) found that people with chronic SCI have altered and weaker ERS/ERD as compared to able-bodied people. Castro et al. (2013) analysed movement related potentials in people with SCI imagining the movement of a paralysed limb. They found that people with SCI have lower readiness and movement related potentials while imagining to move paralysed limbs than able bodied while executing the same movement.

Little is however known how CNP in the presence of SCI affects MRCP. Xu et al. (2014) analysed movement related cortical potential (MRCP) over the central cortical regions covering the primary motor cortex of arms and legs (C3, Cz and C4) in three groups: able bodied, low level injury SCI patients (paraplegia) and low level injury SCI patients with CNP. However, they could not find significant differences between two groups of patients, even though they found differences between able-bodied and SCI patients in general. One of the reason for this is that Xu and colleagues may have missed the macro-scale brain activation patterns because they used only three electrodes. Our recent study, using 61 channels EEG recording system, indicates the influence of CNP on wider cortical structures (Vuckovic et al., 2014). In that study, we analysed ERS/ERD during imagined movements in a group of patients with low level SCI (paraplegia) and CNP and compared them with a group of SCI with no pain and with a group of able-bodied people. We found that CNP resulted in a stronger ERS/ERD in theta, alpha and beta band with characteristic spatial distribution, that were present during the imagination of movement of both painful and non-painful limbs. The group with SCI and no pain had similar but weaker ERS/ERD than the able-bodied group. Thus we showed that it is possible to distinguish the influence of paralysis from the influence of CNP in multichannel ERS/ERD analysis. This leads us to expect that recent developments of EEG analysis using a multivariate signal processing and statistics should allow us to exploit more useful information from the 61-channel EEG data recorded from these patients to further characterize the influence of SCI on CNP.

In the present study, we applied a recently developed Measure Projection Analysis (MPA) (Bigdely-Shamlo et al., 2013), which is a post-processing method after calculating independent component analysis (ICA) and equivalent current dipoles, to determine the influence of SCI on CNP. MPA determines domains, which are defined as clusters of independent components with statistically proximate locations and similarity in measures, i.e. ERP in this case. The novelty of MPA approach is that it enables the analysis of a motor task in terms of functionally rather than spatially distinctive domains. We hypothesise that each functionally distinctive domain will have the characteristic morphology of ERP and that ERPs in different domains might be affected to a different degree by SCI and by CNP.

The advantage of ERP over the ERS/ERD analysis is that it can distinguish between the cognitive, motor, and afferent sensory components by identifying the amplitude, latency and spatial location of the corresponding ERP components. Thus we analysed the effect of CNP and SCI on each component separately. While in Vuckovic et al. (2014) we defined the influence of CNP on different frequency bands, in this study we investigate the effect of CNP on ERP based on different phases of cue-based motor task.

## 2. Material and methods

### 2.1. Participants

Twenty nine people in 3 age matched groups were recruited for the study. Ten Able-Bodied (AB) (3F, 7 M, age 39.1 ± 10.1), 7 people with SCI with CNP (PwP) below the level of injury (1F, 6 male M, age 41.5 ± 8.1) and 8 people with SCI and with no acute or chronic pain (PnP) (3F, 5 M, age 44.7 ± 9.1) participated in the study. The American Spinal Injury Association Impairment (ASIA) classification scale (Kirshblum et al., 2011) was used to determine the neurological level of injury. CNP in SCI patients may be perceived at the level and below the level of injury. Below-level pain is a central pain occurring as a result of the spinal lesion, whereas at-level pain may be caused by spinal cord or root lesion and may therefore have both peripheral and central pain components (Bryce et al., 2012; Finnerup et al., 2014).

PwP patients were asked to fill out a Brief Pain Inventory (Tan et al., 2004) to describe the location and intensity of pain as measured by a visual numerical scale (0 = no pain, 10 = worst pain imaginable). Exclusion criteria for all 3 groups were the self-reported presence of neurological disorders or brain injury which could influence EEG interpretation as well as the presence of any other chronic pain at the time of the experiment.

Inclusion criteria for PwP were either motor and sensory complete (ASIA A) or motor complete and sensory incomplete (ASIA B), with spinal lesion at the level T1 to T12 lasting at least 1 year. They had diagnosed CNP for at least 6 months following SCI (Mehta et al., 2016) with the intensity of pain equal or larger than 5 on the visual numerical scale. Information on CNP medication was not a part of the inclusion/exclusion criteria. It was difficult to recruit patients with moderate to high pain intensity who were not taking medication. PwP participants 1, 3, 4, 5 and 6 used anticonvulsants while patient 7 used antidepressants for treatment of pain, as shown in Table 1.

The inclusion criteria for PnP was similar to PwP: completes of injury ASIA A or B and level of injury T1 to T12 lasting at least 1 year. The demography of PwP and PnP groups is shown in Tables 1 and 2, respectively.

**Table 1**
The demography of the spinal cord injured patients with central neuropathic pain. G: Gabapentin, P: Pregabalin, ASIA: The American Spinal Injury Association. VNS: Visual Numerical Scale.

| No. | Level of injury | ASIA* | Years after injury | Intensity of pain (VNS¥) | Year with pain | Medication |
|---|---|---|---|---|---|---|
| 1 | T5 | A | 7 | 7 | 7 | G, carbamzepine |
| 2 | T5/T6 | A | 11 | 6 | 11 | none |
| 3 | T5 | A | 7 | 8 | 7 | P,G |
| 4 | T7 | B | 6 | 8 | 5 | none |
| 5 | T6/T7 | B | 25 | 10 | 24 | G |
| 6 | T1 | A | 25 | 5 | 10 | P |
| 7 | T5 | A | 14 | 5 | 13 | Amitriptyline |

**Table 2**
The demography of spinal cord injured patients with no central neuropathic pain. ASIA: The American Spinal Injury Association.

| No. | Level of injury | ASIA | Years after injury |
|---|---|---|---|
| 1 | T7 | A | 7 |
| 2 | T7 | B | 7 |
| 3 | T12 | A | 7 |
| 4 | T2 | A | 2 |
| 5 | T5 | B | 15 |
| 6 | T11 | A | 11 |
| 7 | T4 | A | 9 |
| 8 | T7 | A | 15 |

All patients had motor complete injury. The reason for including both sensory complete and incomplete injury (ASIA A and B) was that there is no evidence that either injury level or completeness of injury are related to the incidence of CNP (Siddall et al., 2003). The level of injury might affect the level of cortical reorganisation of the sensory motor cortex of the upper and lower limbs, which might affect MRCP (Lacourse et al., 1999, Castro et al., 2013). From that reason only paraplegic patients were included in the study. Time after injury might also affect MRCP in a similar way as it affects ERD/ERS (López-Larraz et al., 2015), thus only patients with chronic injury were included in the study. Some patients took CNP medications (antidepressants and anticonvulsants) which might have influenced the resting state oscillatory brain activity. Antidepressants increase EEG amplitude in the theta and the higher beta band (>20 Hz) (Wauquier et al., 2005), whereas antiepileptic drugs are known to slow down the dominant frequency and increase the energy in the theta (4–8 Hz) and delta (1–4 Hz) bands (Bauer and Bauer, 2005). Antispastic drugs taken by 1 patient target gamma-aminobutyric acid receptors and could potentially also increase the energy level in the theta and delta bands (Vienne et al., 2012). Our previous study of oscillatory EEG activity in these groups (Vuckovic et al., 2014) showed that PwP group had a comparable level of theta and alpha activity to the AB group, while in PnP that activity was significantly reduced. It is however not know in which way these medications would influence MRCP.

To compare the level of an injury, the level of injury C1 to T12 was assigned numerical values 1 to 21. Years after injury and level of injury were compared among patient groups using Wilcoxon's rank sum test. The analysis showed that there were no significant differences in neither time post injury ($p = 0.5467$) not at the level of injury ($p = 0.2235$). Thus although both complete and incomplete SCI patients were recruited, the completeness of injury comparably affected both groups. That should allow to separate the effect of paralysis from the effect of CNP on MRCP. Analysis of EEG over electrode locations Cz and C3 showed comparable morphology and amplitude of MRCP in patients with and without CNP (Xu et al., 2014)

All participants provided a written informed consent for the study; the study was approved by the National Health Service ethical committee for SCI patients groups and by the University of Strathclyde ethical committee for able-bodied volunteers. The experiments were performed in accordance with the Declaration of Helsinki.

### 2.2. EEG recording

EEG signal was recoded using a 61 channels EEG device (Synamp$^2$, Neuroscan, USA). The electrodes were placed according to the standard 10–10 system (ACNS, 2005). An ear-linked reference was used and an electrode placed at AFz served as ground. The sampling frequency was 1 kHz and the electrode impedance was below 5 kΩ. Electromyograms (EMG) were recorded from the right and the left wrist extensor muscles and the right leg outer gastrocnemius muscle using the bipolar inputs to the Synamp device. The only purpose of EMG recording was to check for the absence of voluntary movements when subjects attempted motor imagery (MI).

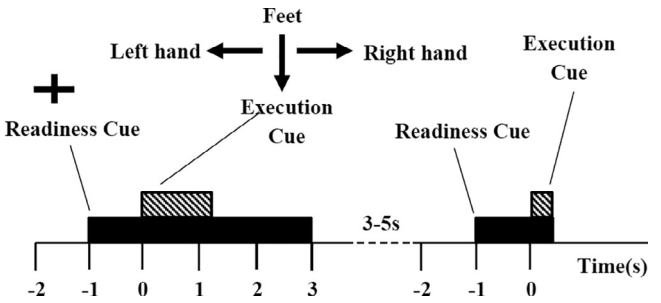


**Fig. 1.** The experimental paradigm. At $t = -1$ s a readiness cue (a cross) appeared at the computer screen. At $t = 0$ s, an execution cue, appeared at the computer screen. It was presented in a form of an arrow pointing to the right, left or down that indicated imagination of movement of the right hand (RH), left hand (LH) or feet (F) accordingly; the execution cue was displayed for 1.25 s.

### 2.3. Experimental setup

Participants were instructed to perform MI tasks which consisted of the imagined waving with their right or left hand or tapping with both feet every time they saw a corresponding visual cue at a computer screen (Fig. 1). Participants were seated at a desk and were facing a computer screen (15″ size) on an approximate distance of 150 cm. At t = −1 s a readiness cue (a cross) appeared at the computer screen giving participants an indication to prepare to imagine a movement. One second later, this was followed by a readiness cue (t = 0), an arrow pointing to the right, left or down, giving participants an indication to imagine movements of their right hand, left hand or feet accordingly; the cue was displayed for 1.25 s. The participants were asked to continuously perform motor imagery till the cross disappeared at t = 3 s. A 3–5 s rest period was given to the participants before the next trial started.

The MI experiment was divided into 6 sub-sessions, and each sub-session took approximately 5 min. Each sub-session contained 30 trials (10 for each movement type in randomised sequences). Therefore, each participant had 60 trials for each type of MI.

### 2.4. Signal pre-processing

EEG was recoded with 1 kHz sampling frequency. EEG signal was divided into epochs, starting at t = −1 s and finishing at t = 3 s (4 s long). The epoched EEG signal was high passed filtered at 0.1 Hz (IIR, 12db cut-off frequency) and a notch filter (48–52 Hz) was also applied in order to remove the line noise (50 Hz). Then, the EEG signal was down-sampled to 250 Hz. The down-sampled EEG signal was exported to EEGLab (Delorme and Makeig, 2004). In EEGLab, the EEG signal was visually inspected and trials containing the amplitude larger than 100 μV over all channels or that were accompanied with EMG were manually rejected. No more than 3–4 trials were rejected per participant. Following this, the EEG signal was re-referenced to an average reference and independent component analysis (ICA) decomposition was performed as described below. IC components containing biological or instrumental noise identified by their characteristic morphology, spatial distribution and frequency content were removed prior to further analysis.

### 2.5. Event related potential measure projection

The method (Bigdely-Shamlo et al., 2013) comprises of:

- ICA decomposition and equivalent dipole localisation.

- Spatial smoothing of a given dynamic measure (in this case ERP) for the equivalent dipole-localised ICs.
- Measure Projection Analysis: this comprises of defining the subspace of brain voxel locations with a significant local IC measures of similarity.
- Creating spatial brain voxel domains which exhibit sufficient measure differences.

*2.5.1. ICA decomposition, equivalent dipole localisation and spatial smoothing*

ICA decomposes EEG from multiple channels into maximally temporary independent components by creating a set of spatial filters *W*. Independent components are then created from EEG using a simple linear transformation

$$S = WX \quad (1)$$

where S is the effective source EEG activation that is decomposed by ICA, W is an unmixing matrix, and X is the observed signal i.e. EEG. The filters *W* have a fixed projection to recording electrodes and produce the maximally independent time courses of data. Thus ICA defines which independent processes contribute to data recorded on a scalp EEG and reveals their independent scalp projections. Some of components represent non-brain 'artefact' sources i.e. 'noise', having either biological (EOG, ECG, EMG) or instrumental (e.g. line noise) origin and can be removed from the ICAs set. To calculate ICs, the Informix algorithm (Bell and Sejnowski, 1995) with the extended-ICA algorithm (Lee et al., 1999) that extracts the mixed sub-Gaussian and super-Gaussian sources effectively was implemented in EEGLab (Delorme and Makeig, 2004).

Following noise removal, the location of dipoles corresponding to remaining ICs were determined for each IC based on the boundary element model (Akalin Acar and Makeig, 2010). A single dipole location procedure was used to estimate the location of the ICs (Zou et al., 2006), as most IC originating from the brain can be modelled by a single dipole (Nunez and Srinivasan, 2006, Delorme et al., 2012). Compared to methods which estimate a dipole location from EEG scalp maps, that presents the mixture of sources. The uncertainty of dipole locations based on ICs is reduced due to a fact that each ICA presents a single source. The set of ICs with a low residual variance (<15%) and with equivalent dipoles located inside the Montreal Neurological Institute (MNI) brain volume were chosen for data analysis. This allowed anatomical location over the cortex and defining the nearest Brodmann Areas (BA), as well as several subcortical areas.

The precise localisation of sources is possible only if a precise head model based on magnetic resonance imaging MRI of that subject is available (Akalin Acar and Makeig, 2010). The level of accuracy in this group analysis was somewhat reduced due to a fact that the cortical locations of multiple subjects were wrapped into a common head model to allow group Measure Projection (MP). Therefore the dipole localisation method may occasionally localize sources deeper than they are really located. A co-registration between channel locations and head model surface was performed to align the dataset channel locations to a three-shell stored Boundary head model template montage, followed by dipoles fitting for the ICs.

A spatial smoothing was performed using a truncated 3-D Gaussian spatial kernel. A standard deviation for each 3-D Gaussian, representing each equivalent dipole location, was set to 28 mm (full width half maximum). This value was recommended by creators of MPA method (Bigdely-Shamlo et al., 2013) and was chosen heuristically to minimize the ambiguity of equivalent dipole localisation arising from numerical inaccuracies, errors in measurement methods and in a head model. Each Gaussian was then truncated to a radius of 3 standard deviations (84 mm) to prevent interfering influences from distant sources.

In this study, common ICs were calculated for EEG of all three conditions together (MI of the right hand, left hand and of both feet) and common dipoles were defined. However, following this step, data from different conditions were separated for Measure Projection Analysis (MPA), because it was expected that they might have a distinctive ERP, different for MI of each motor task.

*2.5.2. Measure projection analysis*

This step is the core of the whole analysis. MPA is a method which compares amongst EEG source locations and dynamics across different subjects and sessions in a 3-D brain space (Bigdely-Shamlo et al., 2013). It is based on a probabilistic approach that treats source-resolved data as samples drawn from the distribution of source locations and dynamics. It focuses on a single dynamic measure (in this case ERP) and performs a statistical analysis on a grid of brain locations rather than on individual sources.

In order to define the subspace of brain voxel locations with significant local IC measures, a brain volume is presented as a cubic dipole source space grid with 8-mm spacing. Voxels outside the MNI brain volume are discarded.

A measure vector $M_i(x)$ is then obtained by vectorising ERP time course associated with each singe IC with an equivalent dipole $D(x)$. Based on this, the method estimates an interpolated measure vector $M(y)$, defined across all possible brain locations $y \in V$, and then estimates the statistical significance (i.e. $p$ value) of this assignment for each of these locations. The $p$ value is associated with a null hypothesis that $M(y)$ has a random spatial distribution in the brain.

Each estimated dipole $D_j$, $j = 1 \ldots n$, is presented by a spherical truncated Gaussian kernel with covariance $\sigma^2 I$ at an estimated dipole location $\hat{x}_j$, where standard deviation $\sigma$ encapsulates dipole localisation errors. The Gaussian is further normalised to ensure that densities in the different areas of a brain volume (e.g. deep inside the brain and closer to the surface) have a unity mass within the brain volume.

A probability that an estimated dipole $D_j$ is truly located at position $j$ is presented by a normalised truncated Gaussian distribution $P_j(y) = TN(y; \hat{x}_j, \sigma^2 \cdot I, t)$. For an arbitrary location, the value of expected (projected) measure vector $M(y)$ is

$$E\{M(y)\} = \langle M(y) \rangle = \frac{\Sigma_{i=1}^{n} P_i(y) M_i}{\Sigma_{i=1}^{n} P_i(y)} = \sum_{i=1}^{n} \bar{P}(y) M_i \quad (2)$$

Where $\bar{P}(y)$(with a property $\Sigma_{i=1}^{n} \bar{P}_i = 1$) is a probability that the estimated location of measure vector $M_i(y)$ is truly M(y).

The next step upon obtaining an estimate measure vector $M(y)$ at each brain voxel location is to test against the null hypothesis that $M(y)$ is produced by a random set of measure vectors $M_i$. The overall goal of this is to identify brain areas, or 'neighborhoods' that exhibit statistically significant similarities in ERP based measure between IC of equivalent dipoles within the neighborhood. To do that it is necessary to calculate the measure of convergence $C(y)$ at each brain location $j \in V$

$$C(y) = E\{S(y)\} = \frac{\Sigma_{i=1}^{n} \Sigma_{j=1, j \neq i}^{n} P_i(y) P_j(y) S_{i,j}}{\Sigma_{i=1}^{n} \Sigma_{j=1, j \neq i}^{n} P_i(y) P_j(y)} \quad (3)$$

where $P_i(y)$ is the probability of dipole $D_i$ being at location $y$, and $P_j(y)$ is the probability of dipole $D_j$ being at location $y$, with an additional assumption that dipoles are independent, in order to factorise a joint probability. A factor $S_{i,j}$ is the degree of similarity associated with dipoles $D_i$ and $D_j$. A convergence $C(y)$ is the expected value of measure similarity at location $y$. The calculated value C is a scalar which is larger in the area of homogenous (similar) ICs.

The recommended measure of the degree of similarity $S_{i,j}$ in MPT toolbox is the signed mutual information *SMI* (Darbellay and Vajda, 1999) between IC-pair ERP measure, which is based on a correlation *CORR* (Bigdely-Shamlo et al., 2013).

$$SMI = \frac{1}{2} sign(CORR) log_2\left(\frac{1}{1 - CORR^2}\right) (bits/sample) \quad (4)$$

Once the significance of *C(y)* is found for each group and each task, they can be compared between tasks or between groups. Different tasks for different groups will be called a condition *c* further in the text.

*2.5.3. ERP domain clustering*

A method chosen for domain clustering in MPT toolbox is the Affinity Propagation Clustering (Frey and Dueck, 2007). The clustering step is only used to determine the granularity of segmentation of brain regions exhibiting significant measure consistency obtained in the previous step and therefore does not change the projected source measure values. It is based on the similarity matrix $S_{nxn}$ of pairwise correlations between *n* measure projection values at each voxel point. This method has the following properties:

1. It does not require an a priori knowledge of the number of clusters. It automatically finds the appropriate number of clusters based on the maximum allowed correlation between the cluster exemplars. It increases the number of clusters until any potential cluster exemplar becomes too similar to the one of the existing exemplars. In this study correlation was set to the recommended value of 0.8 (Bigdely-Shamlo et al., 2013). This means that the maximum allowed correlation between clusters is 0.8. Increasing the correlation value to 0.9 would result in an increased number of clusters of smaller size (but they would cover the same 3D area as clusters in the case of correlation = 0.8). Likewise, reducing correlation to 0.7 would result in the smaller number of clusters of a larger size. For the outlier cluster, a correlation was set to the recommended value of 0.7.
2. Affinity propagation clustering determines outliers during the clustering process. This is achieved by adding an an additional row and column to the pair-wise similarity matrix *S* which now has *n + 1* rows and columns $S_{(n+1)x(n+1)}$. The n + 1st column and row contain a fixed element $T_o$, and each point that is less similar than $T_o \in R$ to any cluster exemplar is assigned to the outlier cluster.
3. Clusters do not have a fixed geometric shape (e.g. a sphere as in k-mean clustering). In addition, spatially discontinuous regions of the brain may belong to the same cluster if they present highly functionally connected areas. Finally, because the MPA method is based on the probabilistic representation of dipole locations, it is not necessary that ICs of each single subject contribute to each domain.

To apply Measure Projection analysis, the Measure Projection Toolbox, which is operated as EEGLab plug-in under MATLAB (The Mathworks, Inc, USA), was used. There were three groups in the study, AB, PwP and PnP. Each group had three experimental conditions, which corresponded to motor imagery of the right hand, left hand and feet. Data were grouped using a study structure in EEGLab for the purpose of further analysis.

*2.5.4. Analysis of individual peaks*

In addition to the statistical analysis of time series, the latency and the amplitude of individual peaks following the execution cue were compared between different groups and conditions. Depending on the morphology of a peak (peaks with or without clearly visible maxima), the peak amplitude or the mean amplitude with respect to the baseline around $t = 0$ s were calculated (Luck et al., 2005) and compared using non-parametric paired Wilcoxon sign rank test between conditions and Wilcoxon rank sum test between groups. For a peak without a clearly defined maxima, for which a mean amplitude was calculated, both latency and duration were determined and compared between groups and conditions. For a peak with clearly identifiable maxima, only latency was calculated. The baseline shift around $t = 0$ s, due to slow rebound of ERP following the warning sign, was removed in all groups by calculating the average value of first 50 ms following the cue (before earliest peaks) and subtracting that value from the ERP to set the baseline (following the execution cue) to zero.

## 3. Results

The results of spatial locations of domains are presented first followed by comparison of ERP between different conditions (tasks and groups). The ERP domains are shown in Fig. 2. Fig. 2a shows spatial locations of all three domains together, relative to each other. Fig. 2b–d shows contributions of all three groups to different domains. It can be noticed that dipoles of all three groups are mixed showing no obvious clustering of one particular group within a domain.

*3.1. Analysis of the spatial locations of domains*

Locations of domains with respect to corresponding BAs are shown in Table 3. BAs contributing with less than 5% are not shown (thus explaining why probabilities do not add up to 100%). Subcortical areas are indicated as being closest to the BAs of interest.

Domain 1 was located within the limbic system and covered three Brodmann areas BA25, BA23 and BA 34. This domain was slightly shifted towards the left hemisphere. The rest of domain 1 covered subcortical structures, brain stem, caudate and putamen but these areas should be interpreted with caution due to a known tendency of the head model used in EEGLab to locate dipoles deeper in the brain.

Domain 2 comprised of BA31 located in the postcental gyrus, the primary somamtosensiry cortex (BA2,3), the primary motor cortex (BA 4), supplementary and premotor cortex (BA6) and parietal cortex BA4. Although domain 2 included two spatially disjointed areas, in fact these areas belonged to the neighboring BA (6,4,2,3).

Most of the domain 3 belonged to the occipital cortex, BA30 and BA 19. The activity of domain 3 was related to visual processing of the cue based motor task.

*3.2. Analysis of ERP*

We first presented ERP morphology in different domains in able-bodied people (Fig. 3a–c) and then compared it with ERP in other two groups. ERP was presented for each domain separately and compared pairwise among three groups for each MI task separately. The latency of all peaks for all groups and domains and for each condition are shown in the Supplementary Material, Tables S1–S3.

Fig. 3a–c shows ERPs in all three domains for a representative MI of the left hand in AB group. We defined clearly visible peaks, present for all three types of motor imagery. Peaks larger than 0 were defined as positive and peaks smaller than 0 as negative. Positive 'peaks' in between two negative peaks staying under 0 were not counted as real peaks. Consecutive positive and negative peaks beard the same numbers which increased consecutively from left to right on the time axis. In Supplementary Material, Tables S1–S3, the latencies of peaks were calculated with respect to the near-

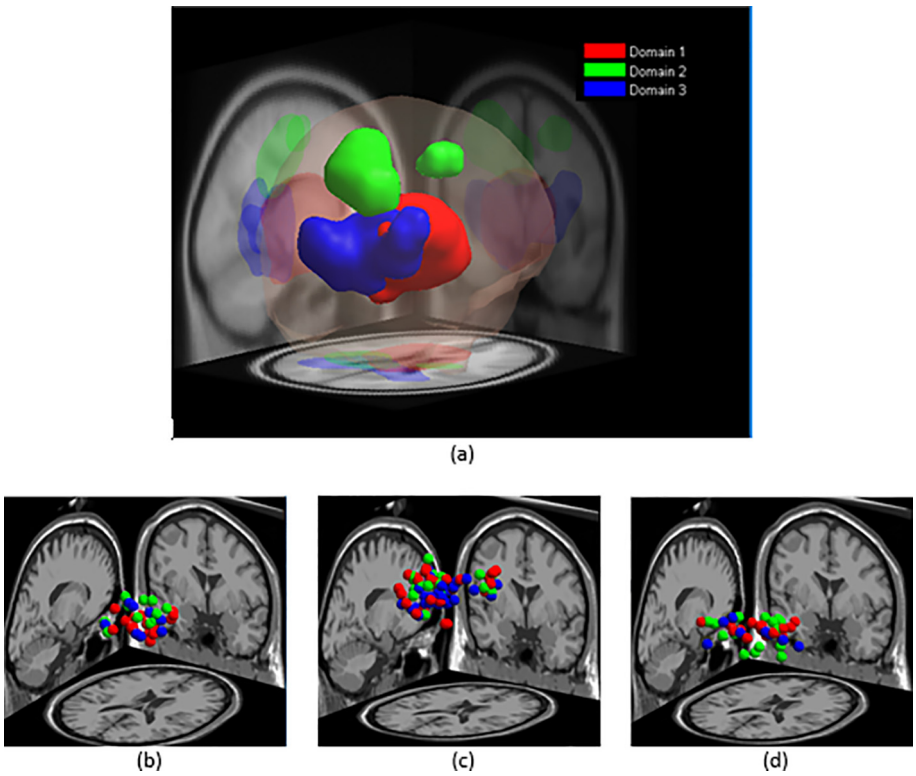


**Fig. 2.** Domains created by MTP (a) all domains together (b) contributions of three groups to domain 1 (c) contribution of three groups to domain 2 (d) contribution of three groups to domain 3. In figure (b–d) red: AB; green: PnP; blue: PwP. (For interpretation of the references to colour in this figure legend, the reader is referred to the web version of this article.)

**Table 3**
BAs contributing to different domains with corresponding probabilities.

| Domain 1 | | Domain 2 | | Domain 3 | |
|---|---|---|---|---|---|
| Location | Probability | Location | Probability | Location | Probability |
| BA 25 | 0.47 | BA 31 | 0.27 | BA 30 | 0.27 |
| BA 23 | 0.16 | BA 3 | 0.17 | BA 19 | 0.24 |
| BA 34 | 0.16 | BA 4 | 0.16 | BA 37 | 0.08 |
| BA 29 | 0.06 | BA 6 | 0.12 | BA 23 | 0.10 |
| BA 28 | 0.06 | BA 40 | 0.08 | BA 27 | 0.07 |
| Caudate | | BA 2 | 0.06 | BA 18 | 0.07 |
| Brainstem | | BA 23 | 0.06 | | |
| Putamen | | | | | |

est event, i.e. the appearance of a warning cue at t = −1 s, the appearance of the execution cue at t = 0 s and the disappearance of the execution cue at t = 1.25 s. Vertical lines in tables delineate between these events.

We start the analysis with domain 2, the part of which included the sensory-motor cortex and is therefore expected to be most similar to ERP analysis of EEG signal over the motor cortex (Xu et al., 2014).

The main difference between EEG derived MRCP and ERP in domain 2 was that ERP in domain 2 was inverted, so positive peaks corresponded to negative peaks in EEG MRCP and vice versa. This was due to IC derived dipole orientation. In a period between the warning and the execution cue, the ERP resembled a contingency negative variation (CNV) in EEG signal preceded by an ERP response to a visual stimulus. The first large, short duration negative peak N1 ($t$ = 170 ms) caused by a visual stimulus was followed by a longer positive peak P1 ($t$ = 300 ms) and a slow negative undershooting (U1) that lasted until the appearance of an execution cue. In a period following the execution cue, a positivity-negativity-positivity complex (P2 at $t$ = 140mn, N2 at $t$ = 200 s and P3 = 330 ms) was followed by an undershooting U2. Peak N2 most likely presented a cognitive response to a visual stimulus, which may have a latency from 100 ms (P100) to 300–400 (P300) (Hillyard and Kutas, 1983) and was also visible with a similar latency in domain 3 located within the visual cortex (Fig. 3, Supplementary Material, Tables S1 and S2). Peak P2 might presented either an early cognitive response to a visual stimuli or, more likely, a "premotor positivity" (Boschert et al., 1983) with the inverted sign. The P2 peak was absent in other two domains, further confirming its relation to the sensory-motor processing. A morphology and latency of peak P3 suggested that it corresponded to an inverted sign motor related potential (MRP) and a negative undershooting (U2) corresponded to the reafferentation potential, having a kinesthetic sensory origin (Botzel et al., 1997).

In domain 1 in a period between the warning and the execution cue, two consecutive brief negative peaks could be noticed (N1 at $t$ = 220 ms and N2 at $t$ = 440 ms) probably as a result of cognitive processing of a visual cue. A typical CNV in domain 1 was absent, unsurprisingly, as CNV originated from BA6 which was the part of domain 2. The morphology of ERP following the execution cue contained a double negativity (N3 at $t$ = 250 ms and N4 at $t$ = 330 ms), followed by a large longer lasting positivity P4 and then another smaller negativity N5. Judging by the post-stimulus latency, N3 and N4 also presented responses to a visual stimulus, probably corresponding to P200 and P300 with inverted signs. Positivity P4 (at $t$ = 720 ms) had a larger latency and was of longer duration than positivity P3 in domain 2 (at $t$ = 340 ms). It most likely corresponded to the reafferentation potential in domain 2, but with an inverted sign. Finally, N5 followed the disappearance of a cue (at $t$ = 1.5 s) with a latency of 255 ms.

ERP in domain 3 covering the occipital cortex had the simplest morphology. In a period following the warning sign a negativity N1 at $t$ = 175 ms was followed by a positivity P1 at $t$ = 265 ms. Follow-

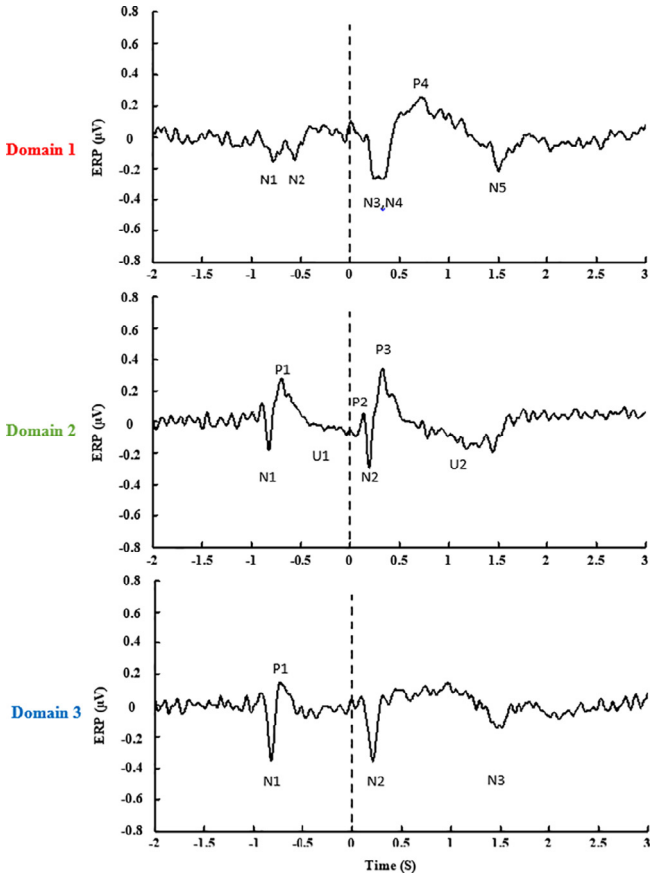


**Fig. 3.** MRCP for AB during MI of the left hand in all three domains. Note that negative peaks below 0, correspond to positive peaks in EEG based ERP. Likewise, positive peaks above 0 correspond to negative peaks in EEG based ERP.

ing an execution cue, a negativity N2 at $t = 210$ ms could be noticed. The morphology and latency of N1, P1 and N2 resembled those of N1, P1 and N2 respectively in domain 2. Finally another negativity at N5 = 260 ms followed disappearance of the execution cue.

Figs. 4–6 show ERP in three groups over three domains, domain 1 Fig. 4a–c, domain 2 Fig. 5a–c and domain 3 Fig. 6a–c. ERPs of all three groups for a single domain and a single type of motor imagery are shown in one graph. For all three domains, ERPs of different types of movement are shown in subplots a–c. Bars under the graphs present nonparametric bootstrap analyses of time series and indicate time instances when ERPs were statistically significant among each of two groups ($p = 0.01$). For each domain, we will first analyse a time period between the warning and the execution cue followed by the analysis of ERP in a period following the execution cue. The analysis of peak amplitude and latencies was performed for a period following the execution cue, for peaks present in all three groups.

In domain 1, following the execution cue, both N1 and N2 could be noticed in PnP and AB group while PwP group had only N1 visible. Similar results could be noticed across all three types of MI because the same warning sign preceded all three types of MI.

In a period following the execution cue, AB and PnP had similar N3, while N4 was significantly delayed in PnP. Group PwP had only N3 while all other peaks were absent. Analysis of peaks was performed for N3 which was visible in all 3 groups. There were no significant differences in N3 latencies, neither between groups nor between conditions. There was no significant difference in the peak amplitude between AB and PnP. However PwP had a significantly smaller peak amplitude than PnP ($p = 0.0235$ feet) and AB ($p = 0.0124$ feet, $p = 4.5672 \cdot 10^{-4}$ left hand).

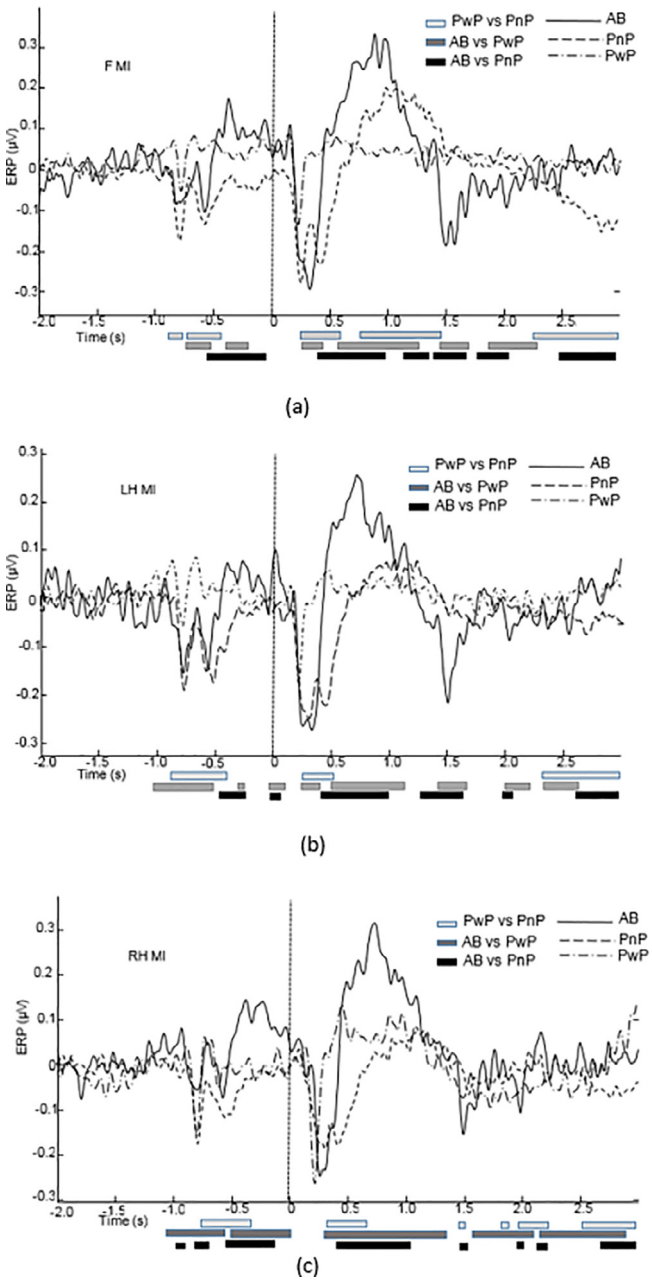


**Fig. 4.** Domain 1 MRCP during motor imagery of Feet: F, Left Hand: LH and Right Hand: RH for three groups AB, PnP and PwP. Thick horizontal lines below the graphs represent the bootstrap statistics and show the intervals with statistically significant differences (p = 0.01) between each pair of groups (a) AB vs PnP, (b) AB vs PwP and (c) PnP vs PwP).

Positivity P4 in AB group was visible for all 3 types of motor imagery, but in PnP group it was noticeable only during MI of feet. Component N5 was visible in AB group only. Consequently, a bootstrap analysis showed a significant difference between AB and PnP, for all three types of MI in a period of N4 and P4 and later during N5. Significant differences between AB and PwP were noticeable throughout the movement (from $t = 0.5$ till $t = 2$ s). Similar to analysis of peaks, bootstrap analysis showed significant differences between PwP and PnP mainly during N3, N4 and P4.

In domain 2, in a period following a warning cue, in PnP group, N1 was very weak or almost absent and P1 returned much slower to the baseline than in AB group; Instead of undershooting, the

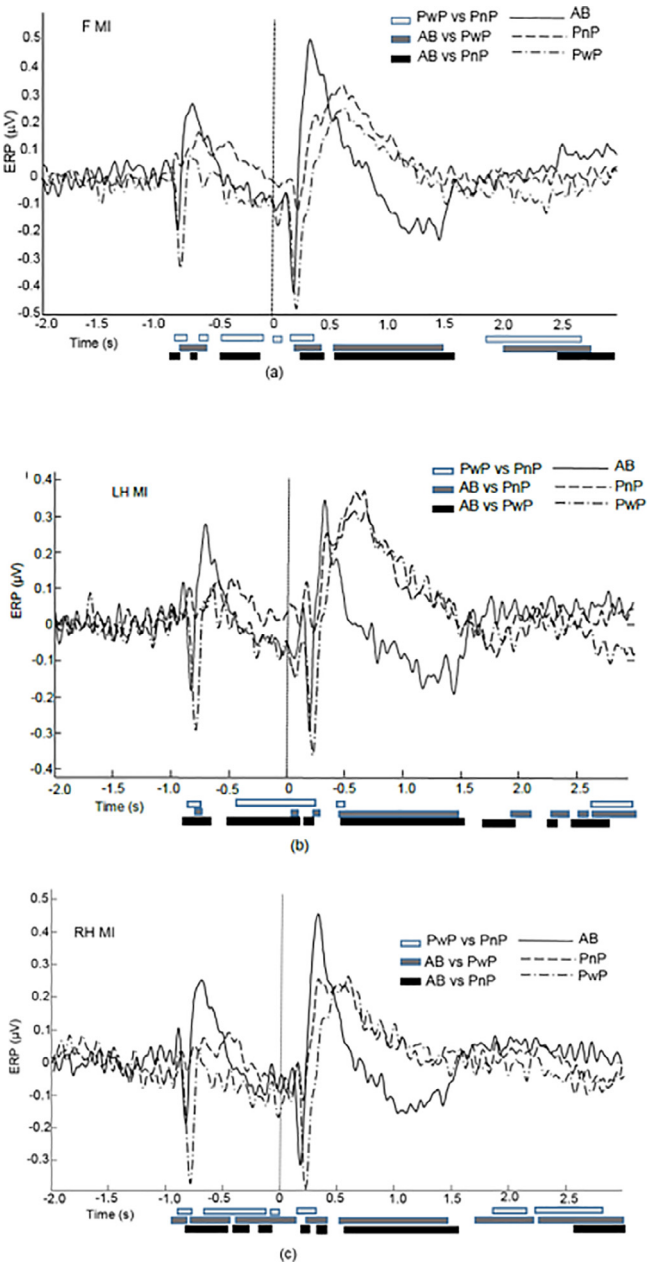


**Fig. 5.** Domain 2 MRCP during motor imagery of Feet: F, Left Hand: LH and Right Hand: RH for three groups AB, PnP and PwP. Thick horizontal lines below the graphs represent the bootstrap statistics and show the intervals with statistically significant differences (p = 0.01) between each pair of groups (a) AB vs PnP, (b) AB vs PwP and (c) PnP vs PwP).

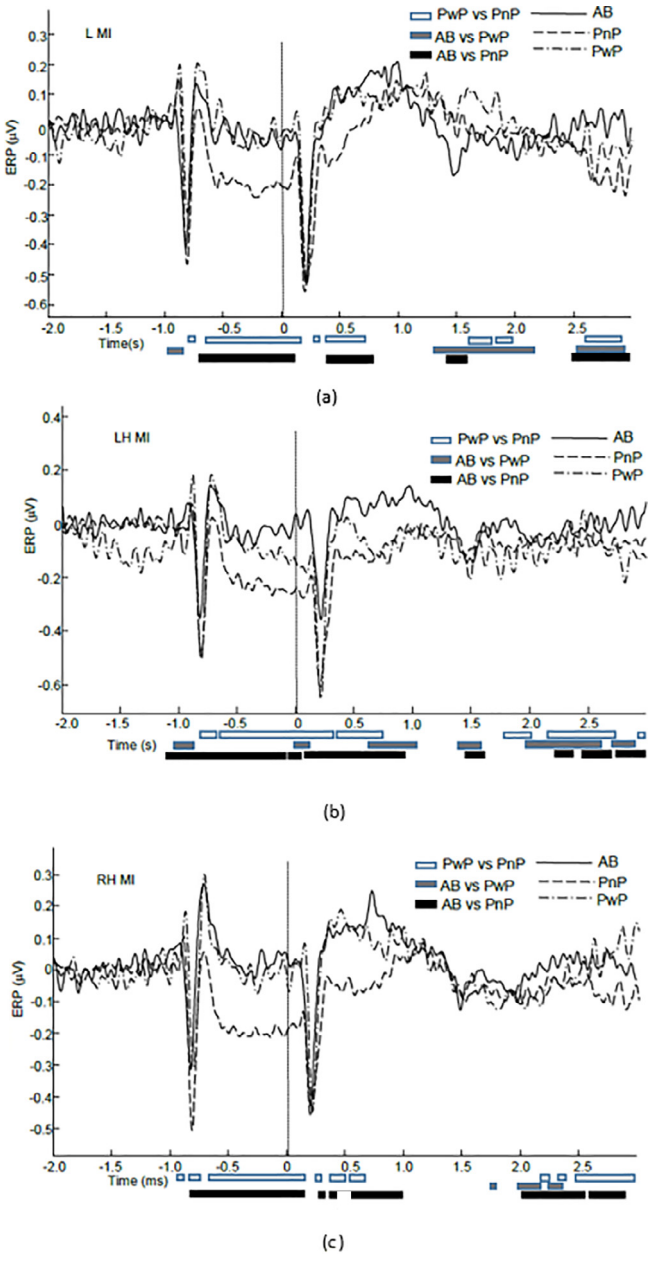


**Fig. 6.** Domain 3 MRCP during motor imagery of Feet: F, Left Hand: LH and Right Hand: RH for three groups AB, PnP and PwP. Thick horizontal lines below the graphs represent the bootstrap statistics and show the intervals with statistically significant differences (p = 0.01) between each pair of groups (a) AB vs PnP, (b) AB vs PwP and (c) PnP vs PwP).

potential was positive following P1 due to slow returning to the baseline value. On the contrary, the morphology of ERP in PwP group was more similar to that of AB but with a significantly larger N1 than in AB group.

In a period following the execution cue, all three groups had visible N2 and P2 but PwP and PnP did not have the undershooting U2, which would correspond to the reafferentation potential in ERP derived from EEG over the motor cortex.

Peak amplitude and latency of P2, N2 and mean amplitude and latency of P3 were compared between groups and conditions. After the baseline correction, there were no statistically significant differences neither in the amplitude nor in the latency of N2 and P2 between different types of MI in any group. No significant difference was found in N2 latency between groups. However PwP had a larger N2 peak than PnP ($p = 2.0037 \cdot 10^{-4}$) and AB group ($p = 0.0148$), and AB had a larger N2 peak than PnP ($p = 0.0023$).

Peak P3 had a larger latency and lasted longer in patient groups as compared to AB. When compared between AB and PnP groups, P3 for MI of feet had a significantly larger latency ($p = 0.017$) and the duration of P3 was significantly longer for PnP group for all three types of MI (feet $p = 0.0034$, right hand $p = 0.0023$, left hand $p = 0.0032$). AB also had a significantly shorter P3 latency than PwP group (feet $p = 8.4872 \cdot 10^{-4}$, right hand $p = 4.3872 \cdot 10^{-4}$) and a significantly shorter duration (feet $p = 3.30245 \cdot 10^{-6}$, right hand $p = 6.4764 \cdot 10^{-4}$, left hand $p = 7.8746 \cdot 10^{-7}$). The duration of P3 was not significantly different between two patient groups and the latency was significantly longer in PwP only for MI of the right hand ($p = 0.0238$). There was no significant difference in the

average amplitude neither between AB and PnP nor between PnP and PwP for any task.

The analysis of P3 latency and duration showed no significant differences between different types of movement for AB group. For PNP group the duration of P3 was not significantly different for different types of MI but P3 had larger latency for MI of feet then of the right hand ($p = 0.0347$). For PwP group, on the contrary, the latency was not significantly different between different types of MI but P3 duration for MI of feet was significantly longer than that of the right hand ($p = 0.0403$).

The bootstrap statistical analysis of ERP time series showed that the whole period between $t = 0.5$ and 1.5 s (movement related potential and reafferentation potential) was significantly different between AB and two patient groups due to larger latencies in patient groups. There was also a significant difference between PwP and other two groups around peak N2 due to the larger N2 amplitude in this group.

In summary, earliest negative peaks in PwP group were significantly larger than in the other two groups. All three groups had similar average amplitude of P3 peak but larger latency, and duration of P3 was larger in patient groups. Apart from the reafferentation potential, EPR had a comparable morphology for all three groups.

In domain 3 the bootstrap analysis showed difference in N2 between PnP and PwP but that was primarily caused by the baseline shift following the warning cue. Subsequent analysis of peaks showed no significant differences in neither the amplitude nor the latency between three groups and three conditions, after baseline correction. In a period following the warning cue, all three groups had N1 and P1 of a comparable latency and intensity (Table 3) but in PnP, the ERP returned slower to the baseline compared to the other two groups. In a period following the execution cue, N2 was also similar in all three groups. Negativity N3 was visible in AB group only, following a disappearance of the execution cue. The largest difference between PnP and the other two groups was not reflected in the amplitudes of peaks but in a slow rebound towards the baseline value. Judging by the latency and morphology of peaks, ERPs in this domain are mostly originating from a visual processing.

## 4. Discussion

Results from the current study revealed three distinctive functional domains which were represented by participants of all three groups comparably. Functional similarity of IC within a domain was expressed in terms of correlation between components. ICs with similar morphology and peak latency were grouped together without an attempt to create a domain of a fixed geometry. Each domain had a distinctive ERP during cue based motor imagery task.

Presence of CNP and of SCI affected domains to a different degree, depending on their function and location. The first domain was located in the limbic cortex and some deeper cortical structures, at least apparently. The limbic system is responsible for regulating sadness and affective component of pain. Almost half of the domain belonged to BA25 which was located in the cingulate cortex and is affecting mood (Mayberg et al., 1999). BA23 was located in the posterior cingulate cortex (PCC), which is amongst the other, involved in the affective component of pain (Nielsen et al., 2005, Jensen, 2010) and is believed to be a part of the Default Mode Network (Leech et al., 2013). There is a functional relation between PCC and BA25 as they both belonged to the Default Mode Network.

A large part of domain 2 belonged to BA 31, a part of the PCC (dorsal posterior cingulate area), which is a part of the limbic system. Other areas of domain 2 involved the primary somatosensory cortex (BA2,3), the primary motor cortex (BA4) and the supplementary and premotor cortices (BA 6), areas of the brain involved in the high level sensory-motor control of movement. Domain 2 also involved BA40, which is responsible for spatial and semantic processing, and was previously found active in cue-based motor imagery tasks (Osuagwu and Vuckovic, 2014). Domain 2 included both the sensory-motor cortex and some parts of the limbic system which in people with CNP regulates the affective component of pain. Thus limbic cortex was distributed between domains 1 and 2.

The third domain was localised within the visual cortex due to a visual nature of the cue based task, and showed well-established and comparable morphology across the three groups. Largest parts of domain 3 belonged to BA 30 and BA 19, the former involving the agranular retrolimbic area, and being responsible for higher cognitive functions, like audio-visual integration and the later involving the associate visual cortex. The latter was also a part of the visual association area (V3) responsible for multimodal integration functions. Because the visual cortex was not the primary target of this study, it was excluded from the following discussion.

The first domain included anatomical areas within the cingulate cortex responsible for the affective component of pain. The ERP of AB and PnP in this domain consisted of early components within the first 400 ms reflecting cognitive processes and late components related to a sensory, reafferentation potential. While PnP had all peaks present but delayed, in PwP group only earliest peaks were present. This indicates a general suppression of ERP related to cognitive and sensory processing. Notably, these peaks were absent not only during motor imagery of painful and paralysed lover limbs but also during motor imagery of non-paralysed and non-painful upper limbs. Pain and paralysis thus had distinctive effects on ERP in the limbic cortex, during cue-based MI task. While paralysis caused delayed responses, the presence of CNP caused ERP suppression similar to the general effect of chronic pain to cognitively related ERP (Maurer et al., 1989, Weisenberg, 1994). Domain 1 showed the largest variability between groups and also to some extend between types of MI in patient groups.

The second domain covered the areas of the primary and secondary sensory and motor cortex. ERP of able-bodied people in this domain looked like inverted EEG MRCP over the primary motor cortex (Xu et al., 2014). In both patient groups, a reafferentation potential was missing, while a component related to movement preparation and execution was present but had a lager latency and lasted longer than in AB group. Earliest peaks were significantly larger in PwP as compared to the other two groups, probably reflecting higher cognitive effort. Motor related potentials were similar in PnP and PwP groups indicating that this component of ERP is probably not influenced by CNP. The absence of the reafferentation potential in this domain (also reported in EEG MRCP (Xu et al., 2014)) in both patient groups might indicate that it is not influenced by CNP. However, considering that a similar ERP component was absent only in PwP group in domain 1, it is more likely that both paralysis and presence of CNP contributed to the reduced processing of kinaesthetic sensory feedback within this domain.

All groups had earliest negative peaks, following the warning and execution cues, visible in all domains and with approximately the same latency both between groups and between domains. There was however a large difference in the amplitude of these peaks in PwP across different domains. In domain 1, a peak flowing the execution cue was significantly smaller in PwP than in the other two groups while it was significantly larger in domain 2. In domain 3 earliest peak was of a comparable amplitude in all three groups. This shows a complex mechanism through which CNP influences cognitive functions. Similar to the effect of the other types of chronic pain on P300 (Maurer et al., 1989, Weisenberg, 1994), the presence of CNP reduced the amplitude of this peak in domain 1, indicating increased habituation. However increased peak in domain 2, which might be an indicator of the lack of

habituation, resembles a phenomena seen in people with neurotic disorders (Miltner et al., 2000), who have increased P300 amplitude when processing stimuli related to critical fear concern, which in this case might be the imagery of the movement of a painful limb.

While this study is restricted to CNP in people with SCI, it would be interesting to know whether similar changes are present in other patient groups suffering from CNP, such as amputees (Floor, 2002), patients after stroke (Andersen et al., 1995), patients with Multiple sclerosis (Osterberg, 2005) and patients with Parkinson's disease (Beiske et al., 2009). For future studies, we suggest that the researchers also employ ICA and MPA to replicate our findings. This research field needs to see more pieces of evidence accumulated from application of these advanced computational approaches.

One limitation of the study is that the accuracy of source localisation was limited by that of equivalent current dipole fittings. There is a known bias toward depth of the brain when applying this method. Because of this tendency, we sometimes observed apparent localisation results within basal, and cerebellar regions, from which scalp-observable EEG signals are unlikely to be generated due to their citoarchitectures. Care needs to be taken to interpret these results, and the apparent deep-brain sources are, for now, better interpreted to be closer to the surface along with radial projection lines to the surface.

Another possible limitation of study is validity in one of the processes in MPA. MPA first uses ERP measure, in the case of current study, to create consistent domains, then tests their differences across conditions. This way of using the same data twice is known to inflate a bias toward false positives, a problem known as 'double dipping' (Vul et al., 2009). Unfortunately, there is neither analytical nor empirical analysis to quantifying this bias in MPA, so it is hard to determine how much it influences the current result. However, there are at least two reasons why the use of it does not have to be excluded. One reason is that according to the principle of human functional brain mapping, ICs localised within a certain region should show naturally correlated activation patterns even without using constraint of similarity of measures. This is a different situation from what Vul and colleagues criticised in the social cognitive neuroscience studies, where sociocognitive scores were directly correlated to BOLD signal data. The other reason is that the number of ICs is much smaller than the number of voxels in fMRI: 100–1000 ICs divided into 5–10 domains vs. whole-brain 200,000 voxels. From these comparisons, we believe that the situation in MPA is more benign than that of sociocognitive fMRI studies in question, and the estimated demerit of using MPA does not exclude the use of it.

## 5. Conclusions

CNP had the largest influence on ERP in a domain which included the limbic system with no contribution from the sensory-motor cortex. In the domain including sensory-motor cortex MRCP of both patients groups was similar and delayed as compared to the able bodied. Smallest differences existed in a domain which included the visual cortex. Both pain and paralysis affected the reafferentation potential while CNP influenced cognitive processes in a manner that depended on the functional domain.

## 6. Conflict of interest

None.

## Acknowledgements

This work was supported by the MRC grant G0902257/1, NED University of Pakistan PhD scholarship and a PhD Scholarships by the High Committee for Education Development, Iraq. We would like to thank Professor Bernard Conway, University of Strathclyde for lending EEG equipment, and to the creator of MPT method Dr Nima Bidgely Shamlo on the clarification of Domain localisation.

## Appendix A. Supplementary material

Supplementary data associated with this article can be found, in the online version, at https://doi.org/10.1016/j.clinph.2018.05.020.

## References

Akalin Acar Z, Makeig S. Neuroelectromagnetic forward head modeling toolbox. J Neurosci Methods 2010;190:258.
American Clinical Neurophysiology Society. Guideline 5 Guidelines for standard electrode position nomenclature. J Clin Neurophysiol 2005;23:107–10.
Andersen G, Vestergaard K, Ingeman-Nielsen M, Jensen TS. Incidence of central post-stroke pain. Pain 1995;61:187–93.
Bauer G, Bauer R. EEG, drug effects and central neural system poisoning. In: Niedermeyer E, da Silva L, editors. Electroencephalography, basic principle, clinical applications and related fields. Philadelphia: Lippincott Williams & Wilkins; 2005. p. 701–23.
Beiske AG, Loge JH, Rønningen A, Svensson E. Pain in Parkinson's disease: prevalence and characteristics. Pain 2009;141:173–7.
Bell AJ, Sejnowski TJ. An information-maximization approach to blind separation and blind deconvolution. Neural Comput 1995;7:1129–59.
Bigdely-Shamlo N, Mullen T, Kreutz-Delgado K, Makeig S. Measure projection analysis: a probabilistic approach to EEG source comparison and multi-subject inference. NeuroImage 2013;72:287–303.
Boord P, Siddall PJ, Tran Y, Herbert D, Middleton J, Craig A. Electroencephalographic slowing and reduced reactivity in NP following spinal cord injury. Spinal Cord 2008;46:118–23.
Boschert J, Hink RF, Deecke L. Finger movement versus toe movement-related potentials: further evidence for supplementary motor area (SMA) participation prior to voluntary action. Exp Brain Res 1983;52:73–80.
Bötzel K, Ecker C, Schulze S. Topography and dipole analysis of reafferent electrical brain activity following the Bereitschafts potential. Exp Brain Res 1997;114:352–61.
Bryce TN, Biering-Sorensen F, Finnerup NB, Cardenas DD, Defrin R, Lundeberg T, Norrbrink C, Richards JS, Siddall PJ, Stripling T, Treede RD, Waxman SG, Widerstrom-Noga E, Yezierski RP, Dijkers M. International spinal cord injury pain (ISCIP) classification. Part I. Background and description. Spinal Cord 2012;50:413–7.
Castro A, Díaz F, Sumich A. Long-term neuroplasticity in spinal cord injury patients: a study on movement-related brain potentials. Int J Psychophysiol 2013;87:205–14.
Darbellay G, Vajda I. Estimation of the information by an adaptive partitioning of the observation space. IEEE Trans Inf Theor 1999;45:1315–21.
Delorme A, Makeig S. EEGLAB: an open source toolbox for analysis of single-trial EEG dynamics including independent component analysis. J Neurosci Methods 2004;13:9–21.
Delorme A, Palmer L, Onton J, Oostenveld R, Makeig S. Independent EEG sources are dipolar. Plos One 2012;7:e30135.
Finnerup NB, Norrbrink C, Trok K, Piehl F, Johannesen IL, Sørensen JC, Jensen TS, Werhagen L. Phenotypes and predictors of pain following traumatic spinal cord injury: a prospective study. J Pain 2014;15:40–8.
Floor H. Phantom-limb pain: characteristics, causes, and treatment. Lancet Neurol 2002;1:182–9.
Frey BJ, Dueck D. Clustering by passing message between data points. Science 2007;315:972.
Jensen MP. A neuropsychological model of pain: research and clinical implications. J Pain 2010;11:2–12.
Hillyard SA, Kutas M. Electrophysiology of cognitive processing. Annu Rev Psychol 1983;34:33–61.
Jensen TS, Baron R, Haanpää M, Kalso E, Loeser JD, Rice AS, Treede RD. A new definition of neuropathic pain. Pain 2011;52:2204–5.
Kirshblum SC, Burns SP, Biering-Sorensen F, Donovan W, Graves DE, Jha A, et al. International standards for neurological classification of spinal cord injury (revised 2011). J Spinal Cord Med 2011;34:535–46.
Lacourse MG, Cohen MJ, Lawrence KE, Romero DH. Cortical potentials during imagined movements in individuals with chronic spinal cord injuries. Behav Brain Res 1999;104:73–88.
Lee TW, Girolami M, Sejnowski TJ. Independent component analysis using an extended infomax algorithm for mixed subgaussian and supergaussian sources. Neural Comput 1999;11:417–41.
Leech R, Braga R, Sharp DJ. Echoes of the brain within the posterior cingulate cortex. The J Neurosci 2013;32:215–22.

López-Larraz E, Montesano L, Gil-Agudo Á, Minguez J, Oliviero A. Evolution of EEG motor rhythms after spinal cord injury: a longitudinal study. PLoS One 2015;10:e0131759.
Luck S. An introduction to the event-related potential technique. In: An introduction to event-related potentials and their neural origin. MIT Press; 2005. p. 1–50.
Maurer K, Riederer P, Heinsen H, Beckmann H. Altered P300 topography due to functional and structural disturbances in the limbic system in dementia and psychoses and to pharmacological conditions. Psychiatry Res 1989;29:391–3.
Mayberg HS, Liotti M, Brannan SK, McGinnis S, Mahurin RK, Jerabek PA, et al. Reciprocal limbic-cortical function and negative mood: converging PET findings in depression and normal sadness. Am J Psychiatry 1999;156:675–82.
Mehta S, Guy SD, Bryce TN, Craven BC, Finnerup NB, Hitzig SL, et al. The CanPain SCI clinical practice guidelines for rehabilitation management of neuropathic pain after spinal cord: screening and diagnosis recommendations. Spinal Cord 2016;2016(54):S7–S13.
Miltner WHR, Krieschel S, Gutberlet I. P300–a signature for threat processing in phobic subjects. Psychophysiology 2000;37:71.
Nielsen FA, Balslev D, Hansen LK. Mining the posterior cingulate: segregation between memory and pain components. Neuroimage 2005;27:520–32.
Nunez PL, Srininvasan R. Electric fields in the brain: the neurophysics of EEG. Oxford University Press; 2006.
Osuagwu BA, Vuckovic A. Similarities between explicit and implicit motor imagery in mental rotation of hands: an EEG study. Neuropsychologia 2014;65:197–210.
Osterberg A, Boivie J, Thuomas KA. Central pain in multiple sclerosis-prevalence and clinical characteristics. Eur J Pain 2005;9:531–42.
Pfurtscheller G, Lopes da Silva F. Event-related EEG/MEG synchronization and desynchronization: basic principles. Clin Neurophysiol 1999;110:1842–57.
Pfurtscheller G, Linortner P, Winkler R, Korisek G, Müller-Putz G. Discrimination of motor imagery-induced EEG patterns in patients with complete spinal cord injury. Comput Intell Neurosci 2009;104180.
Siddall PJ, McClelland JM, Rutkowski SB, Cousins MJ. A longitudinal study of the prevalence and characteristics of pain in the first 5 years following spinal cord injury. Pain 2003;103:249–57.
Shibasaki H, Barrett G, Halliday E, Halliday AM. Components of the movement-related cortical potential and their scalp topography. Electroencephalogr Clin Neurophysiol 1980;49:213–26.
Tan G, Jensen MP, Thornby JI, Shanti BF. Validation of the brief pain inventory for chronic nonmalignant pain. J Pain 2004;5:133–7.
Vienne J, Lecciso G, Constantinescu I, Schwartz S, Franken P, Heinzer R, Tafti M. Differential effects of sodium oxybate and baclofen on EEG, sleep, neurobehavioral performance, and memory. Sleep 2012;35:1071–83.
Vuckovic A, Hasan MA, Fraser M, Conway BA, Nasseroleslami B, Allan DB. Dynamic oscillatory signatures of central neuropathic pain in spinal cord injury. J Pain 2014;15:645–55.
Vul E, Harris C, Winkielman P, Pashler H. Puzzling high correlations in fMRI studies of emotions, personality and social cognition. Former title (Voodoo Correlations in Social Neuroscience). J Assoc Psychol Sci 2009;4:274–90.
Wauquier A. EEG and neuropharmacology. In: Niedermeyer E, da Silva L, editors. Electroencephalography, basic principle, clinical applications and related fields. Philadelphia: Lippincott Williams & Wilkins; 2005. p. 689–700.
Weisenberg M. Cognitive aspects of pain. In: Wall PD, Melzack R, editors. Textbook of pain. Edinburg: Churchill-Livingstone; 1994. p. 275–89.
Xu R, Jiang N, Vuckovic A, Hasan M, Mrachacz-Kersting N, Allan D, et al. Movement-related cortical potentials in paraplegic patients: abnormal patterns and considerations for BCI-rehabilitation. Front Neuroeng 2014;27:7–35.
Zou L, Zhu S, He B. ICA-based EEG spatio-temporal dipole source localization: a model study. In: Wang J, Yi Z, Zurada J, Lu B, Yin H, editors. Advances in Neural Networks. China: Springer; 2006. p. 566–72.